Carcinogenesis Advance Access published April 24, 2013
Carcinogenesis

OXFORD JOURNALS
Carcinogenesis

Grape antioxidant dietary fiber (GADF) inhibits intestinal polyposis in $Apc^{Min/+}$ mice: relation to cell cycle and immune response

Journal:	*Carcinogenesis*
Manuscript ID:	CARCIN-2012-01066.R2
Manuscript Type:	Original Manuscript
Date Submitted by the Author:	21-Feb-2013
Complete List of Authors:	Sánchez-Tena, Susana; University of Barcelona, Biochemistry and Molecular Biology Lizárraga, Daneida; Maastricht University, Department of Health Risk Analysis and Toxicology Miranda, Anibal; University of Barcelona, Biochemistry and Molecular Biology Vinardell, Maria; University of Barcelona, Phisiology García-García, Francisco; Centro de Investigación Príncipe Felipe (CIPF), Department of Bioinformatics Dopazo, Joaquín; Centro de Investigación Príncipe Felipe (CIPF), Department of Bioinformatics Torres, Josep; Institute for Advanced Chemistry of Catalonia (IQAC-CSIC), Institute for Advanced Chemistry of Catalonia (IQAC-CSIC) Saura-Calixto, Fulgencio; Institute of Food Science and Technology and Nutrition (ICTAN-CSIC), Department of Metabolism and Nutrition Capella, Gabriel; Institut Català d'Oncologia (ICO)-IDIBELL, Translational Research Laboratory Cascante, Marta; University of Barcelona, Biochemistry and Molecular Biology
Keywords:	Grape, Dietary Fiber, Colon cancer, Cell cycle, Immune response

Grape antioxidant dietary fiber (GADF) inhibits intestinal polyposis in Apc$^{Min/+}$ mice: relation to cell cycle and immune response

Susana Sánchez-Tena[1,2], Daneida Lizarraga[3], Anibal Miranda[1,2], Maria Pilar Vinardell[4], Francisco García-García[5,6,7], Joaquín Dopazo[5,6,7], Josep Lluís Torres[8], Fulgencio Saura-Calixto[9], Gabriel Capellà[10] and Marta Cascante[1,2,*].

[1]Department of Biochemistry and Molecular Biology, Faculty of Biology, Universitat de Barcelona, Barcelona, Spain; [2]Institute of Biomedicine of Universitat de Barcelona (IBUB) and Unit Associated with CSIC, Barcelona, Spain; [3]Department of Health Risk Analysis and Toxicology, Maastricht University, Maastricht, The Netherlands; [4]Departament de Fisiologia, Facultat de Farmacia, Universitat de Barcelona, Barcelona, Spain; [5]Functional Genomics Node, National Institute of Bioinformatics, Centro de Investigación Príncipe Felipe (CIPF), Valencia, Spain; [6]Department of Bioinformatics, CIPF, Spain; [7]CIBER de Enfermedades Raras (CIBERER), Valencia, Spain; [8]Institute for Advanced Chemistry of Catalonia (IQAC-CSIC), Barcelona, Spain; [9]Department of Metabolism and Nutrition, Institute of Food Science and Technology and Nutrition (ICTAN-CSIC), Madrid, Spain; [10]Translational Research Laboratory, IDIBELL-Catalan Institute of Oncology, Barcelona, Spain

[*]To whom correspondence should be addressed: Department of Biochemistry and Molecular Biology, Faculty of Biology, Universitat de Barcelona, Av. Diagonal, 643. 08028 Barcelona, Spain. Phone: 34-934021593; Fax: 34-934021559; E-mail: martacascante@ub.edu

Running title: Grape antioxidant dietary fiber inhibits polyposis

Abstract

Epidemiological and experimental studies suggest that fiber and phenolic compounds might have a protective effect on the development of colon cancer in humans. Accordingly, we assessed the chemopreventive efficacy and associated mechanisms of action of a lyophilized red grape pomace containing proanthocyanidin-rich dietary fiber (Grape Antioxidant Dietary Fiber, GADF) on spontaneous intestinal tumorigenesis in the $Apc^{Min/+}$ mouse model. Mice were fed a standard diet (control group) or a 1% (w/w) GADF-supplemented diet (GADF group) for 6 weeks. GADF supplementation greatly reduced intestinal tumorigenesis, significantly decreasing the total number of polyps by 76%. Moreover, size distribution analysis showed a considerable reduction in all polyp size categories [diameter <1 mm (65%), 1–2 mm (67%) and >2 mm (87%)]. In terms of polyp formation in the proximal, middle and distal portions of the small intestine a decrease of 76%, 81% and 73% was observed respectively. Putative molecular mechanisms underlying the inhibition of intestinal tumorigenesis were investigated by comparison of microarray expression profiles of GADF-treated and non-treated mice. We observed that the effects of GADF are mainly associated with the induction of a G1 cell cycle arrest and the down-regulation of genes related to the immune response and inflammation. Our findings show for the first time the efficacy and associated mechanisms of action of GADF against intestinal tumorigenesis in $Apc^{Min/+}$ mice, suggesting its potential for the prevention of colorectal cancer.

Introduction

Most grape dietary fibre and phenolics accumulate in the fruit skins, seed and pulp, which after the manufacture of grape juice and wine remains as pomace. After production, this processed raw material becomes a by-product and is used as fertilizer, animal feed or disposed in dumps, being a great waste of health-promoting compounds. As there is some evidence suggesting that dietary intake of vegetables and fruits, rich in fibre and phenolic compounds, is associated with a decrease in the risk of developing colorectal cancer [1], further study of these by-products may help to define their application as colon cancer chemopreventive agents.

Grape Antioxidant Dietary Fiber (GADF), here in the form of lyophilized red grape pomace, is a wine processing by-product from red grape that is rich in dietary fibre and phenolics. It contains a large amount (13% w/w) of non-extractable polymeric proanthocyanidins (PA), mainly (epi)catechin-based polymers that are part of the dietary fiber fraction together with lignins and polysaccharides. During its transit along the intestinal tract, the small soluble phenolics are absorbed and the remaining PA progressively release (epi)catechin units that are then absorbed and metabolized. The remaining polymeric PA are cleaved by the intestinal microbiota into smaller species such as phenolic acids, which in turn are absorbed and metabolized [2]. Previous studies in male Wistar rats have shown that GADF reduces mucosal apoptosis, probably due to modulation of the gluthathione redox system and endogenous antioxidant enzymes [3]. Recently, Lizárraga and colleagues reported that the inclusion of GADF in the mouse diet protects the normal colon tissue against polyp development through alterations in the expression of tumor suppressor genes and proto-oncogenes as well as the modulation of enzymes pertaining to the xenobiotic detoxifying system and endogenous antioxidant cell defenses [4]. Together, these results suggest that GADF could be an effective chemopreventive agent against colorectal cancer. However, the efficacy of GADF as a chemopreventive agent needs to be established in well-defined preclinical models of colon cancer before embarking on clinical trials.

The $Apc^{Min/+}$ mouse is a model of colon cancer that harbors a dominant germline mutation at codon 850 of the homolog of the human adenomatous polyposis coli (*Apc)* gene, which results in a defective protein product that predisposes the mice to spontaneously develop pre-neoplastic intestinal polyps [5]. APC function is linked to the Wnt signaling pathway, in which it operates by activating β-catenin degradation. Therefore, mutation of the *Apc* gene produces cytosolic accumulation and an increase in the nuclear translocation of β-catenin. In the nucleus, β-catenin activates the transcription factor T cell factor/lymphoid enhancer factor (TCF/LEF), giving rise to an increase in the expression of genes regulating cell proliferation and predisposing the cells to the formation of tumors. Mutations in the *Apc* gene have been directly implicated in the development of both human familial adenomatous polyposis (FAP) and sporadic colorectal cancer [6]. Hence, the $Apc^{Min/+}$ mouse model is considered an analog of human intestinal tumorigenesis and has been widely used to study the effects of dietary and pharmaceutical agents on human colon cancer prevention. Here we assessed the efficacy and associated molecular mechanisms of action of GADF consumption on spontaneous intestinal tumorigenesis in $Apc^{Min/+}$ mice.

Materials and methods

Grape antioxidant dietary fiber (GADF)

GADF was obtained from red grapes (the *Cencibel* variety) harvested in the vintage year 2005 in *La Mancha* region in Spain, as described in the Spanish patents registered under the numbers 2259258 and 2130092. The percentage composition of GADF used in this work was as follows: dietary fiber, 73 ± 0.8 (58 ± 0.8 comprising an indigestible fraction of insoluble compounds such as lignin and proanthocyanidins and 16 ± 0.1 of a soluble fraction constituted by pectins and hemicellulose); polymeric proanthocyanidins associated with insoluble dietary fiber, 15 ± 0.2; fat, 8 ± 0.5; protein, 11 ± 0.5 and ash, 5 ± 0.2. More than 100 phenolic compounds (not associated with dietary fiber) such as phenolic acids, anthocyanidins, catechins and other flavonoids have been detected in GADF [7].

Animals and diet

We used male $Apc^{Min/+}$ mice aged 5 weeks from Jackson Laboratories (Bangor, ME). Animals were housed in plastic cages at 22 °C and 50% humidity, with a 12:12 h light/dark cycle, according to European Union Regulations. The experimental protocols were approved by the Experimental Animal Ethical Research Committee of the University of Barcelona in accordance with current regulations for the use and handling of experimental animals. After 7 days of acclimatization during which they received a standard diet (Teklad Global 18% Protein rodent diet), the animals were randomly divided into two groups, with 12 and 10 mice per group (Control and GADF respectively). Control mice continued to be fed the standard diet, and the GADF-treated group was fed a special diet comprising the basal diet (Teklad Global 18% Protein rodent diet) supplemented with GADF at 1% w/w, that mimicked the recommended dietary fiber intake for humans [8]. Diets were purchased from Harlan Interfauna Iberica S.L (Barcelona, Spain). Both food and water were supplied *ad libitum* throughout the experiment. Throughout the 6-week treatment period, mice were observed for any signs of toxicity, and body weight and food and water intake were recorded weekly. At the end of the 6 weeks, the animals were starved overnight and then anesthetized with volatile isoflurane (Esteve, Barcelona, Spain). Finally, animals were sacrificed by an overdose of anesthesia.

Measurement of intestinal polyps

Apc$^{Min/+}$ mice develop polyps in both the small and large intestine, although more intestinal adenomas are observed in the small intestine. Therefore, after sacrifice, the small intestine was excised from each mouse. Immediately after sacrifice, the small intestine was cut longitudinally and rinsed with phosphate-buffered saline solution (pH 7.4) to remove the intestinal contents. The intestines were pinned flat on cardboard and then fixed for 1 day in 4% neutral buffered formalin solution (v/v; pH 7.4). Intestinal sections were stored at room temperature in 1% neutral buffered formalin solution (v/v) until further analysis. In order to facilitate tumor quantification and identification, the small intestine was divided into three equal sections: proximal, medial and distal. Thereafter the small intestine sections were stained in phosphate-buffered saline solution (pH 7.4) and 0.1% (v/v) methylene blue. Using a stereomicroscope and a measured grid, the number of tumors and their dimensions in each small intestine section were determined. The size of each tumor was categorized as <1 mm, 1–1.9 mm, or ≥2 mm.

RNA isolation and gene profiling by Affymetrix Microarrays

Large intestine was removed and placed on a plastic plate, which was kept at 4 °C on ice. After removal of the rectum, the colon was opened longitudinally with fine scissors, and mucus, feces and polyps were removed. The normal colonic mucosal layer was incubated in Trizol (Invitrogen, Carlsbad, CA) for 3 min and scraped off the muscle layer using the edge of a sterile glass slide. Cells were transferred into 800 µl Trizol, homogenized by pipetting, and stored at -80 °C until RNA isolation. Total RNA was isolated using a combination of the Trizol method (Invitrogen, Carlsbad, CA) and the RNeasy Mini kit and DNase I treatment (Qiagen, Germantown, MD) according to the manufacturer´s protocols. RNA integrity was tested using lab-on-a-chip technology on the BioAnalyzer 2100 (Agilent, Palo Alto, CA, USA) and only a RNA integrity number (RIN) > 8 was accepted. Affymetrix Microarrays using the Mouse Genome 430 2.0 platforms were performed according to the protocols published by the manufacturer (Affymetrix). We analyzed five RNA samples chosen at random from each group, five for the control and five for GADF group.

Microarray data analyses

Data were standardized using the Robust Multi-array Average method [9] and quantile normalization. Differential gene expression was assessed using the *limma* [10] package from Bioconductor. Multiple testing adjustment of p-value was conducted according to Benjamini and Hochberg [11]. Biochemical pathway analysis was conducted using the Kyoto Encyclopedia of Genes and Genomes (KEGG) Mapper. This is a collection of KEGG mapping tools for KEGG pathway mapping. The tool "Search&Color Pathway" was used to overlay gene expression results from microarrays onto biochemical pathways found in the KEGG. Gene expression levels were denoted using color codes displayed along the pathway by gene symbol boxes. Different shapes and patterns were used to represent induced and suppressed gene expression. Enrichment analysis was based on MetaCore™, an integrated knowledge database and software suite for pathway analysis of experimental data and gene lists. Enrichment analysis consists of matching the gene IDs of possible targets for the "common", "similar" and "unique" sets with gene IDs in functional ontologies in MetaCore. The probability of a random intersection between a set of IDs the size of the target list with ontology entities is estimated by the p-value of the hypergeometric intersection. A lower p-value means higher relevance of the entity to the dataset, which results in higher rating for the entity. Use of the False Discovery Rate (adjusted p-value) allows processes with doubtful significance for the current experiment to be rejected, and ensures that the findings are not contaminated with false positives.

RT-real time PCR

One microgram of total RNA was reverse transcribed following the instructions of the manufacturer (Invitrogen). The cDNA product was used for subsequent amplification by real time PCR in an ABI Prism 7000 Sequence Detection System using gene-specific primers following the manufacturer's recommendations (Applied Biosystems). β2 microglobulin (B2M) RNA was used as an internal control.. Fold-changes in gene expression were calculated using the standard ΔΔCt method.

Results

GADF supplementation inhibits spontaneous intestinal polyposis without affecting body weight in APC$^{Min/+}$ mice

During the experiment the body weight and food and water consumption of all mice were monitored. Food consumption and body weight gain did not differ between the control and GADF groups throughout the study and no mortality was observed in any group (data not shown). GADF treatment did not result in macroscopic changes indicative of toxicity in any organs including the liver, lung and kidney.

GADF supplementation significantly decreased the total number of small intestine tumors by 76%. Control mice developed an average of 16 polyps per animal and GADF treatment decreased this number to 3.9 (Figure 1A). Moreover, as shown in Figure 1B, GADF treatment induced a decrease in the number of small intestine polyps in the proximal, medial and distal sections of 76% (4.6 ± 0.9 versus 1.1 ± 0.3), 81% (4.3 ± 1.0 versus 0.8 ± 0.3) and 73% (7.3 ± 2.4 versus 2.0 ± 0.4) respectively. Analysis of the size distribution of polyps revealed that GADF reduced the occurrence or growth of <1 mm diameter polyps by 65% (5.5 ± 1.2 versus 1.9 ± 0.4), of 1–2 mm by 67% (3.0 ± 1.1 versus 1.0 ± 0.3) and of >2 mm by 87% (7.7 ± 2.2 versus 1.0 ± 0.3) (Figure 1C).

Gene expression profile induced by GADF

To elucidate the underlying mechanisms by which GADF prevents carcinogenesis we determined the transcriptional profile of the Apc$^{Min/+}$ mouse colonic mucosa following GADF treatment using cDNA microarrays.

Of the 39,000 genes represented on the whole mouse genome cDNA microarray, 183 genes were differentially expressed between the control and GADF groups with a 1.5-fold change or more in expression. Of these 183 differentially expressed genes, 40 genes were up-regulated and 143 genes were down-regulated. A complete list of these differentially expressed genes is shown in supplemental table 1.

This list of differentially expressed genes associated with GADF consumption was subjected to a KEGG molecular pathway analysis using KEGG Mapper to identify any enrichment of genes with specific biological themes. Figure 2 presents the differentially expressed genes detected in the KEGG cell cycle pathway analysis using KEGG Mapper. GADF treatment led to a reduction in the expression of the *Ccnd1* gene, which codes for cyclin D, which in turn is involved in regulating cell cycle progression and drives the G1/S phase transition. Moreover, an increase in the expression of a regulator of this protein called *Gadd45a* was detected. The GADD45 protein interacts with many effectors, such as Cdk1/CyclinB, PCNA (which regulates Cyclin D/Cdk4,6), and p21, thus mediating cell cycle arrest, differentiation or apoptosis [12]. Additionally, the DNA replication pathway represented in KEGG Mapper (data not shown) was also down-regulated in the mucosa of Apc$^{Min/+}$ mice treated with GADF due to inhibition of the expression of *Pold2* and *Rfc1*, two members of the DNA polymerase complex.

KEGG Mapper analysis also showed the modulation of other genes related to cancer pathways (Figure 3). GADF supplementation down-regulated the expression of *Kitl*, which encodes the ligand of the tyrosine-kinase receptor KIT. The ligand for KIT is known as kit ligand or stem cell factor (SCF). Furthermore, study of cancer-related pathways showed that the expression of *Tgfb1* was also down-regulated. TGFβ is a secreted protein that controls a diverse set of cellular processes, including cell proliferation, recognition, differentiation, apoptosis, hematopoesis, angiogenesis, immune functions, chemotaxis and specification of developmental fate.

As mentioned earlier, $Apc^{Min/+}$ mice possess a mutation in the *Apc* gene that results in defective Wnt signaling. The representation of the differentially expressed genes detected in the KEGG Mapper Wnt signaling pathway (Figure 4) showed that GADF down-regulates the expression of *Csnk1e*, which encodes the CKI protein epsilon (CKIε). Wnt signaling has long been regarded as the signaling pathway playing a central role in the intestinal epithelial cell differentiated state; however, recent studies have shown that Notch signaling is also indispensable for this process [13]. In this sense, it is noteworthy that GADF treatment also down-regulated *Lfng* (data not shown), which encodes Fringe, a glycosyltransferase that is involved in the elongation of O-ligands in the Notch pathway [14].

Pathway analysis performed using KEGG Mapper was complemented with an independent analysis by MetaCore to obtain the p-value of each pathway. Pathway analysis of significantly modulated genes using MetaCore showed significant changes in maps that contain several canonical pathways. Table 1 presents the top Maps according to Metacore, showing the greatest down-regulation in the cell cycle, immune system responses and G-protein signaling, whereas cell adhesion was up-regulated. In addition to the above-mentioned cell-cycle-associated genes, Metacore analysis identified up-regulation of the

PLK3, a protein that has been negatively correlated with the development of certain cancers, including colon cancer [15]. Metacore analysis also revealed the down-regulation of immune-system-related genes such as *Lck, Nfkbie, Cxcr4, H2-Ab1, Igh, Igl-V1,* and *Igkv1-117* by GADF. A promoting effect of GADF on enterocytic differentiation was shown by the up-regulation of genes related to cell adhesion molecules such as *Ocln, Cldn4* and *Epha2* in polarized epithelial cells.

Validation of microarray data by RT-PCR

The changes in mRNA expression observed in the microarrays for *Ccnd1*, *Kitl, Csnk1e, Lfng* and *Cxcr4* were further validated by RT-real time PCR (Figure 5). These targets were selected for RT-real time PCR analysis based on their participation in the pathways that were significantly modulated by GADF supplementation.

Discussion

GADF treatment induced a 76% reduction in intestinal polyposis with respect to the control (Figure 1). Interestingly, GADF exerted a higher anti-tumoral effect than observed in previous studies in Apc$^{Min/+}$ mice in similar conditions using dietary fiber or other phenolic compounds. For example, administration of 1% dibenzoylmethane reduced the total number of small intestinal tumors by 50% in Apc$^{Min/+}$ mice [16] and a reduction in small intestinal tumors of only 25% was observed after intake of a greater content of dietary fiber

[17]. It is important to note that the decrease in the number of polyps was homogeneous throughout the small intestine. GADF contains a complex mixture of phenolics including monomers of catechins, anthocyanins, flavonols and hydroxycinnamic acids, as well as (epi)catechin oligomers and polymers (PA), all of which are associated with a fiber matrix of both soluble and insoluble polymers such as polysaccharides and lignins that may influence the absorption of the putatively bioactive GADF components. Small phenolics such as phenolic acids and monomeric (epi)catechins that are originally contained within the matrix are absorbed in the small intestine. In previous publications we described that during transit along the intestinal tract some of the GADF's PA may be partially depolymerized into (epi)catechin monomers and some fermented by the intestinal microbiota and absorbed in the form of smaller phenolic acids [18,19]. The fact that GADF exerts its anti-tumorigenic function homogeneously throughout the intestine could thus be related to the putatively bioactive phenolic compounds embedded in the fiber that are gradually released and absorbed. On the other hand, the size distribution analysis of polyps revealed that GADF inhibits both the appearance and development of intestinal polyps, although the most important inhibitory effect was observed in larger polyps indicating a major inhibition in polyp's progression.

Putative molecular mechanisms underlying the inhibition of intestinal tumorigenesis were investigated by comparison of microarray expression profiles of GADF-treated and non-treated mice. KEGG Mapper analysis mainly showed modifications in cancer-related pathways. Concretely, KEGG cell cycle pathway analysis (Figure 2) suggested that GADF suppresses tumorigenesis in Apc$^{Min/+}$ mice by inducing a G1 cell cycle arrest through cyclin D down-regulation and GADD45 up-regulation. These results are consistent with previous studies in which dietary supplementation with grape seed extract in Apc$^{Min/+}$ mice was found to down-regulate Cyclin D1 and up-regulate Cip1/p21 in small intestinal tissue samples according to immunohistochemical analysis [20]. Likewise, another study reported that grape seed extract up-regulates p21, leading to G1 cell cycle arrest [21]. Additionally, inhibition of DNA synthesis, by down-regulation of *Pold2* and *Rfc1*, may also be involved in the induction of G1 arrest in the cell cycle [22]. In this regard it is worth mentioning that GADF produces a change in mucosal epithelial turn-over favoring cell differentiation and cell death over proliferation by means of stopping cell cycle progression without affecting cell death processes.

Moreover, down-regulation of kit ligand by GADF (Figure 3) may be related to the inhibition of intestinal polyp growth since it has been described that SCF-KIT signaling enhances proliferation and invasion in KIT-positive colorectal cancer cell lines [23]. Another down-regulated gene, TGFβ, has been reported to be involved in the progression of colorectal cancer, and therefore a reduction in its expression suggests higher sensitivity to anti-growth signals and a reduction in angiogenesis [24,25].

KEGG Wnt signaling pathway analysis (Figure 4) showed the inhibition of CKIε, a positive regulator of beta-catenin-driven transcription that is specifically required for the proliferation of breast cancer cells with activated beta-catenin [26]. Interestingly, an important gene under the transcriptional activation induced by β-catenin/TCF/LEF, *cyclin D*, was also down-regulated by GADF antagonizing the deregulated Wnt signaling pathway in Apc$^{Min/+}$ mice. Recent data indicate that Wnt and Notch signaling might play an equally important role in the maintenance of the undifferentiated state of *Apc*-deficient cells [13]. In fact, it has been reported that Notch signaling occurs downstream of Wnt through β-catenin-mediated transcriptional activation of the Notch-ligand Jagged1 [27], suggesting that Notch is an alternative target for the treatment of *Apc*-mutant intestinal polyposis. The inhibition of Fringe, involved in the Notch pathway, suggests that GADF inhibits colon cancer growth through the simultaneous down-regulation of Wnt and Notch signaling.

Inflammation and immune system responses have been reported to have dual effects in cancer, either by providing protection from tumor cells or, when inflammation becomes chronic, by promoting tumor growth. Grape phenolic compounds have been implicated in strengthening immune function [28], but their anti-inflammatory and immune-attenuating properties have recently attracted much attention [29,30]. These functions may play an important role in $Apc^{Min/+}$ mice since the tumorigenesis initiated by intrinsic defects in pathways regulating cell proliferation, as observed in $Apc^{Min/+}$ mice, is driven by repeated inflammation and excessive immune signaling [31]. Accordingly, a study identifying genes involved in tumorigenesis in $Apc^{Min/+}$ mice revealed the up-regulation of various immune system and inflammation genes [32]. Therefore, in this case, diminished immune signaling by GADF (Table 1) may reduce tumor progression. Interestingly, apart from the immuno-attenuating properties of grape phenolics mentioned above, a recent investigation concluded that high fiber intake may be inversely associated with the presence of a cytokine pro-inflammatory profile [33]. Therefore, attenuation of the immune response in $Apc^{Min/+}$ mice treated with GADF could be due to the combined effect of soluble phenolics, insoluble PA and other components of the dietary fiber fraction such as polysaccharides and lignins.

In addition to modulation of the immune response, some of the down-regulated immune system/inflammation genes identified in the Metacore analysis have been associated with tumoral progression. For example, *Cxcr4,* a chemokine receptor specific for stromal cell-derived factor-1, has been reported to be involved in tumorigenicity in breast, pancreatic and colorectal cancer [34-36]. Regarding colorectal cancer, the expression of both stromal cell-derived factor-1 and its receptor CXCR4 has been reported to predict lymph node metastasis. Therefore, lower expression of this protein in GADF-fed mice may be related to the inhibition of tumor growth. GADF supplementation also modulated the expression of *Nfkbie,* which has been reported to regulate cell viability and proliferation during transformation [37]. Additionally, *Lck*, a Src-related tyrosine kinase that is expressed in certain tumors such as human colon carcinoma [38], was down-regulated in the mucosa of $Apc^{Min/+}$ mice treated with GADF.

Interestingly, studies evaluating the consumption of GADF by normal C57BL/6J mice showed many changes in the expression of genes involved in antioxidant activity and xenobiotic metabolism. GADF up-regulated genes encoding enzymes implicated in phase I (biotransformation) of the xenobiotic metabolism that convert hydrophobic compounds to more water-soluble moieties, as well as genes from phase II (detoxifying metabolism) that catalyze several conjugation reactions, and genes encoding for peroxiredoxins, members of the family of mammalian proteins that neutralize reactive oxygen species [4]. Surprisingly, in $Apc^{Min/+}$ mice, GADF had no significant effect on the antioxidant and detoxifying machinery, apart from up-regulation of the *Cyp2c54* gene (supplemental table 1) which encodes a cytochrome P450, demonstrating the importance of the regulation of cell growth and maintenance functions to the detriment of antioxidant and xenobiotic systems in tumor progression.

We hypothesize that the changes in the gene expression profile induced in the intestinal mucosa of Apc$^{Min/+}$ mice treated with GADF and the associated inhibition of spontaneous intestinal polyposis may be a result of the action of phenolic compounds (both soluble and insoluble fiber-like PA) and other components of the dietary fiber fraction. It is likely that the phenolics contained in GADF act through molecular mechanisms such as the modulation of gene expression, as previously reported [39]. On the other hand, although the amount of fiber is little (0.75 %), it may perhaps act via the short chain fatty acids (SCFA) released from their fermentation by the gut microbiota. SCFA are mainly used as an energy source by the intestinal epithelium, but they also have been reported to modulate gene expression in several *in vitro* studies [40,41].

In summary, the present study shows for the first time that dietary administration of GADF prevents spontaneous intestinal polyposis in the Apc$^{Min/+}$ mouse model. The cancer chemopreventive effects of GADF were mainly related to the modulation of cancer progression-related genes, suggesting the induction of G1 cell cycle arrest and the down-regulation of genes related to the immune response and inflammation, and thus a protective effect against chronic inflammation and excessive immune signaling in Apc$^{Min/+}$ mice. The powerful anti-tumoral effect of GADF may be the result of synergy between the different compounds in the dietary fiber, including soluble and insoluble grape phenolics and insoluble polysaccharides and lignins. The fact that GADF is a by-product of the wine industry makes it of particular economic and health interest. Taken together, our findings show that GADF is a promising nutraceutical for the prevention of colon cancer in high-risk populations.

Acknowledgements

The authors thank Miquel Borràs, Joaquín de Lapuente, Javier González and Joan Serret from CERETOX and Gemma Aiza and Francesc Xavier Sanjuan for support in the experiments. Financial support was provided by grants SAF2008-00164, AGL2006-12210-C03-02/ALI and AGL2009-12374-C03-03/ALI from the Spanish government Ministerio de Ciencia e Innovación and personal financial support (FPU program); from the Ministerio de Educación y Ciencia and from the Red Temática de Investigación Cooperativa en Cáncer, Instituto de Salud Carlos III, Spanish Ministry of Science and Innovation & European Regional Development Fund (ERDF) "Una manera de hacer Europa" (ISCIII-RTICC grants RD06/0020/0046). It has also received financial support from the AGAUR-Generalitat de Catalunya (grant 2009SGR1308, 2009 CTP 00026 and Icrea Academia award 2010 granted to M. Cascante), and the European Commission (FP7) ETHERPATHS KBBE-grant agreement nº22263.

References

1. Forte, A., *et al.* (2008) Dietary chemoprevention of colorectal cancer. *Ann Ital Chir*, **79**, 261-7.

2. Tourino, S., *et al.* (2011) Metabolites in Contact with the Rat Digestive Tract after Ingestion of a Phenolic-Rich Dietary Fiber Matrix. *J Agric Food Chem*.

3. Lopez-Oliva, M.E., *et al.* (2010) Grape antioxidant dietary fibre reduced apoptosis and induced a pro-reducing shift in the glutathione redox state of the rat proximal colonic mucosa. *Br J Nutr*, **103**, 1110-7.

4. Lizarraga, D., *et al.* (2011) A Lyophilized Red Grape Pomace Containing Proanthocyanidin-Rich Dietary Fiber Induces Genetic and Metabolic Alterations in Colon Mucosa of Female C57BL/6J Mice. *J Nutr*.

5. Su, L.K., *et al.* (1992) Multiple intestinal neoplasia caused by a mutation in the murine homolog of the APC gene. *Science*, **256**, 668-70.

6. Hinoi, T., *et al.* (2007) Mouse model of colonic adenoma-carcinoma progression based on somatic Apc inactivation. *Cancer Res*, **67**, 9721-30.

7. Tourino, S., *et al.* (2008) High-resolution liquid chromatography/electrospray ionization time-of-flight mass spectrometry combined with liquid chromatography/electrospray ionization tandem mass spectrometry to identify polyphenols from grape antioxidant dietary fiber. *Rapid Commun Mass Spectrom*, **22**, 3489-500.

8. Ferguson, L.R. (2005) Does a diet rich in dietary fibre really reduce the risk of colon cancer? *Dig Liver Dis*, **37**, 139-41.

9. Bolstad, B.M., *et al.* (2003) A comparison of normalization methods for high density oligonucleotide array data based on variance and bias. *Bioinformatics*, **19**, 185-93.

10. Smyth, G.K. (2004) Linear models and empirical bayes methods for assessing differential expression in microarray experiments. *Stat Appl Genet Mol Biol*, **3**, Article3.

11. Benjamini, Y., *et al.* (2001) Controlling the false discovery rate in behavior genetics research. *Behav Brain Res*, **125**, 279-84.

12. Hoffman, B., *et al.* (2009) Gadd45 modulation of intrinsic and extrinsic stress responses in myeloid cells. *J Cell Physiol*, **218**, 26-31.

13. Reedijk, M., *et al.* (2008) Activation of Notch signaling in human colon adenocarcinoma. *Int J Oncol*, **33**, 1223-9.

14. Chen, J., *et al.* (2001) Fringe modulation of Jagged1-induced Notch signaling requires the action of beta 4galactosyltransferase-1. *Proc Natl Acad Sci U S A*, **98**, 13716-21.

15. Dai, W., *et al.* (2002) Down-regulation of PLK3 gene expression by types and amount of dietary fat in rat colon tumors. *Int J Oncol*, **20**, 121-6.

16. Shen, G., *et al.* (2007) Chemoprevention of familial adenomatous polyposis by natural dietary compounds sulforaphane and dibenzoylmethane alone and in combination in ApcMin/+ mouse. *Cancer Res*, **67**, 9937-44.

17. Mutanen, M., *et al.* (2000) Beef induces and rye bran prevents the formation of intestinal polyps in Apc(Min) mice: relation to beta-catenin and PKC isozymes. *Carcinogenesis*, **21**, 1167-73.

18. Tourino, S., *et al.* (2009) Phenolic metabolites of grape antioxidant dietary fiber in rat urine. *J Agric Food Chem*, **57**, 11418-26.

19. Saura-Calixto, F., *et al.* (2010) Proanthocyanidin metabolites associated with dietary fibre from in vitro colonic fermentation and proanthocyanidin metabolites in human plasma. *Mol Nutr Food Res*, **54**, 939-46.

20. Velmurugan, B., *et al.* (2010) Dietary feeding of grape seed extract prevents intestinal tumorigenesis in APCmin/+ mice. *Neoplasia*, **12**, 95-102.

21. Kaur, M., *et al.* (2011) Grape seed extract upregulates p21 (Cip1) through redox-mediated activation of ERK1/2 and posttranscriptional regulation leading to cell cycle arrest in colon carcinoma HT29 cells. *Mol Carcinog*.

22. Takeda, D.Y., *et al.* (2005) DNA replication and progression through S phase. *Oncogene*, **24**, 2827-43.

23. Yasuda, A., *et al.* (2007) Stem cell factor/c-kit receptor signaling enhances the proliferation and invasion of colorectal cancer cells through the PI3K/Akt pathway. *Dig Dis Sci*, **52**, 2292-300.

24. Langenskiold, M., *et al.* (2008) Increased TGF-beta 1 protein expression in patients with advanced colorectal cancer. *J Surg Oncol*, **97**, 409-15.

25. Narai, S., *et al.* (2002) Significance of transforming growth factor beta1 as a new tumor marker for colorectal cancer. *Int J Cancer*, **97**, 508-11.

26. Kim, S.Y., *et al.* (2010) CK1epsilon is required for breast cancers dependent on beta-catenin activity. *PLoS One*, **5**, e8979.

27. Rodilla, V., *et al.* (2009) Jagged1 is the pathological link between Wnt and Notch pathways in colorectal cancer. *Proc Natl Acad Sci U S A*, **106**, 6315-20.

28. Katiyar, S.K. (2007) UV-induced immune suppression and photocarcinogenesis: chemoprevention by dietary botanical agents. *Cancer Lett*, **255**, 1-11.

29. Kawaguchi, K., *et al.* (2011) Effects of antioxidant polyphenols on TNF-alpha-related diseases. *Curr Top Med Chem*, **11**, 1767-79.

30. Misikangas, M., *et al.* (2007) Three Nordic berries inhibit intestinal tumorigenesis in multiple intestinal neoplasia/+ mice by modulating beta-catenin signaling in the tumor and transcription in the mucosa. *J Nutr*, **137**, 2285-90.

31. Saleh, M., *et al.* (2011) Innate immune mechanisms of colitis and colitis-associated colorectal cancer. *Nat Rev Immunol*, **11**, 9-20.

32. Leclerc, D., *et al.* (2004) ApcMin/+ mouse model of colon cancer: gene expression profiling in tumors. *J Cell Biochem*, **93**, 1242-54.

33. Chuang, S.C., *et al.* (2011) The intake of grain fibers modulates cytokine levels in blood. *Biomarkers*, **16**, 504-10.

34. Holm, N.T., *et al.* (2009) Elevated chemokine receptor CXCR4 expression in primary tumors following neoadjuvant chemotherapy predicts poor outcomes for patients with locally advanced breast cancer (LABC). *Breast Cancer Res Treat*, **113**, 293-9.

35. Wang, Z., *et al.* (2008) Blockade of SDF-1/CXCR4 signalling inhibits pancreatic cancer progression in vitro via inactivation of canonical Wnt pathway. *Br J Cancer*, **99**, 1695-703.

36. Yoshitake, N., *et al.* (2008) Expression of SDF-1 alpha and nuclear CXCR4 predicts lymph node metastasis in colorectal cancer. *Br J Cancer*, **98**, 1682-9.

37. Dooley, A.L., *et al.* (2011) Nuclear factor I/B is an oncogene in small cell lung cancer. *Genes Dev*, **25**, 1470-5.

38. Krystal, G.W., *et al.* (1998) Lck associates with and is activated by Kit in a small cell lung cancer cell line: inhibition of SCF-mediated growth by the Src family kinase inhibitor PP1. *Cancer Res*, **58**, 4660-6.

39. Yun, J.W., *et al.* (2010) Characterization of a profile of the anthocyanins isolated from Vitis coignetiae Pulliat and their anti-invasive activity on HT-29 human colon cancer cells. *Food Chem Toxicol*, **48**, 903-9.

40. Hu, S., *et al.* (2011) The microbe-derived short chain fatty acid butyrate targets miRNA-dependent p21 gene expression in human colon cancer. *PLoS One*, **6**, e16221.

41. Mangian, H.F., *et al.* (2009) Butyrate increases GLUT2 mRNA abundance by initiating transcription in Caco2-BBe cells. *JPEN J Parenter Enteral Nutr*, **33**, 607-17; discussion 617.

Table 1. Pathways modified in the colon mucosa of $Apc^{Min/+}$ mice by GADF treatment as found in Metacore

GeneGO Maps/Modulated pathways	$^{\$}$p-value	‡Significant/total genes
Cell cycle and its regulation (↓)		
Regulation of G1/S transition (part 1) (↓)	0,0010	2 (*Ccnd1, Tgfb1*)/38
Nucleocytoplasmic transport of CDK/Cyclins (↓)	0,0023	1 (*Ccnd1*)/14
ATM / ATR regulation of G2 / M checkpoint (↑)	0,0005	2 (*Gadd45a, Plk3*)/26
Immune response (↓)		
CXCR4 signaling via second messenger (↓)	0,0007	3 (*Lck, Nfkbie, Cxcr4*)/34
TCR and CD28 co-stimulation in activation of NF-kB (↓)	0,0012	3 (*H2-Ab1, Nfkbie, Lck*)/40
ICOS pathway in T-helper cell (↓)	0,0017	3 (*H2-Ab1, Nfkbie, Lck*)/46
NFAT in immune response (↓)	0,0023	4 (*H2-Ab1, Nfkbie, Lck, Ig*)/51
T cell receptor signaling pathway (↓)	0,0025	3 (*H2-Ab1, Nfkbie, Lck*)/52
G-protein signaling (↓)		
G-Protein alpha-q signaling cascades (↓)	0,0007	3 (*Rgs2, Plcb4, Nfkbie*)/34
Proinsulin C-peptide signaling (↓)	0,0025	3 (*Ccnd1, Plcb4,Nfkbie*)/52
Cell adhesion (↑)		
Tight junctions (↑)	0,0010	2 (*Ocln, Cldn4*)/36
Ephrin signaling (↑)	0,0016	1 (*Epha2*)/45

More significantly modulated pathways in Metacore using genes with FC>1.5 and adjusted p-value<0.01. ↑/↓, activation/inhibition of the biological process by GADF; $^{\$}$p-value that corresponds to the GeneGO Map/Pathway. ‡Ratio between the number of significantly modulated genes by GADF (indicated between parentheses) and the total number of genes per GenenGO Map/Pathway in Metacore.

Figure legends

Fig. 1. A) Total number of polyps/mouse in the small intestine of Apc$^{Min/+}$ mice. B) Number of polyps/mouse in proximal, medial and distal sections. C) Number of polyps/mouse shown by polyp size distribution (<1 mm diameter polyps, 1–2 mm and >2 mm). Data represented as mean ± SEM (*, p > 0.05) (* *, p > 0.01).

Fig. 2. Adaptation of KEGG cell cycle pathway using KEGG Mapper. Oval pathway members were significantly down-regulated and rectangular members were found to be up-regulated in the intestinal mucosa of Apc$^{Min/+}$ mice treated with GADF. Horizontal lines indicate a fold change (FC) of between 1.5 and 2.

Fig. 3. Adaptation of KEGG pathways in cancer using KEGG Mapper. Ovals represent down-regulated genes following GADF supplementation. Horizontal lines indicate a FC of between 1.5 and 2 and vertical lines specify a FC of more than 2.

Fig. 4. Adaptation of KEGG Wnt signaling pathway using KEGG Mapper. Ovals represent down-regulated genes encoding that protein in Apc$^{Min/+}$ mice following GADF treatment. Horizontal lines indicate a FC in expression of between 1.5 and 2 and vertical lines specify a FC of more than 2.

Fig. 5. Validation of genes that were differentially expressed in the colon mucosa of Apc$^{Min/+}$ mice after GADF treatment by RT-PCR. Data represented as mean ± SEM (* *, p > 0.01).

Supplemental table 1. Differentially expressed genes by GADF treatment in the colon mucosa of APC$^{Min/+}$ mice

Affimetrix ID	Gene Symbol	Gene description	Fold change	Adjusted p-value
1418283_at	Cldn4	claudin 4	2,0	0,047
1449133_at	Sprr1a	small proline-rich protein 1A	2,0	0,035
1451924_a_at	Edn1	endothelin 1	1,9	0,049
1419911_at	Coro1c	coronin, actin binding protein 1C	1,8	0,047
1443208_at			1,8	0,035
1441115_at	D18Ertd232e	DNA segment, Chr 18, ERATO Doi 232, expressed	1,8	0,041
1439124_at	Wdr91	WD repeat domain 91	1,8	0,049
1417133_at	Pmp22	peripheral myelin protein 22	1,7	0,022
1433205_at	Ndfip2	Nedd4 family interacting protein 2	1,7	0,039
1436520_at	Ahnak2	AHNAK nucleoprotein 2	1,7	0,044
1436750_a_at	Oxct1	3-oxoacid CoA transferase 1	1,7	0,049
1424339_at	Oasl1	2'-5' oligoadenylate synthetase-like 1	1,7	0,036
1455180_at	Gcom1	GRINL1A complex locus	1,7	0,047
1455457_at	Cyp2c54	cytochrome P450, family 2, subfamily c, polypeptide 54	1,7	0,049
1436614_at			1,7	0,046
1430191_at	9130004J05Rik	RIKEN cDNA 9130004J05 gene	1,7	0,045
1434496_at	Plk3	polo-like kinase 3 (Drosophila)	1,7	0,022
1458279_at			1,7	0,022
1455804_x_at	Oxct1	3-oxoacid CoA transferase 1	1,6	0,049
1422823_at	Eps8	epidermal growth factor receptor pathway substrate 8	1,6	0,044
1441030_at	Rai14	retinoic acid induced 14	1,6	0,044
1426818_at	Arrdc4	arrestin domain containing 4	1,6	0,035
1437868_at	Fam46a	family with sequence similarity 46, member A	1,6	0,035
1435059_at	Asap1	ArfGAP with SH# domain, ankyrin repeat and PH domain1	1,6	0,036

1436101_at	Pank2	pantothenate kinase 2 (Hallervorden-Spatz syndrome)	1,6	0,047
1438581_at	Cytsa	cytospin A	1,6	0,047
1425837_a_at	Ccrn4l	CCR4 carbon catabolite repression 4-like (S. cerevisiae)	1,6	0,049
1417732_at	Anxa8	annexin A8	1,6	0,049
1421151_a_at	Epha2	Eph receptor A2	1,6	0,035
1439598_at			1,5	0,036
1458591_at	Rasef	RAS and EF hand domain containing	1,5	0,044
1417335_at	Sult2b1	sulfotransferase family, cytosolic, 2B, member 1	1,5	0,049
1452385_at	Usp53	ubiquitin specific peptidase 53	1,5	0,044
1449519_at	Gadd45a	growth arrest and DNA-damage-inducible 45 alpha	1,5	0,050
1448873_at	Ocln	occludin	1,5	0,044
1455033_at	Fam102b	family with sequence similarity 102, member B	1,5	0,047
1426894_s_at	Fam102a	family with sequence similarity 102, member A	1,5	0,049
1435265_at			1,5	0,035
1458453_at	Lmo7	LIM domain only 7	1,5	0,048
1422824_s_at	Eps8	epidermal growth factor receptor pathway substrate 8	1,5	0,049
1418459_at	Ccdc91	coiled-coil domain containing 91	-1,5	0,035
1420249_s_at	Ccl6	chemokine (C-C motif) ligand 6	-1,5	0,049
1449342_at	Ptplb	protein tyrosine phosphatase-like (proline instead of catalytic arginine), member b	-1,5	0,047
1452191_at	Prcp	prolylcarboxypeptidase (angiotensinase C)	-1,5	0,047
1430514_a_at	Cd99	CD99 antigen	-1,5	0,044
1430656_a_at	Asnsd1	asparagine synthetase domain containing 1	-1,5	0,049

1435864_a_at	1810063B05Rik	RIKEN cDNA 1810063B05 gene	-1,5	0,047
1451091_at	Txndc5	thioredoxin domain containing 5	-1,5	0,049
1433831_at	4833418A01Rik	RIKEN cDNA 4833418A01 gene	-1,5	0,047
1422029_at	Ccl20	chemokine (C-C motif) ligand 20	-1,5	0,049
1451987_at	Arrb2	arrestin, beta 2	-1,5	0,035
1428340_s_at	Atp13a2	ATPase type 13A2	-1,5	0,039
1453550_a_at	Far1	fatty acyl CoA reductase 1	-1,5	0,036
1436038_a_at	Pigp	phosphatidylinositol glycan anchor biosynthesis, class P	-1,5	0,049
1434955_at	March1	membrane-associated ring finger (C3HC4) 1	-1,5	0,049
1421022_x_at	Acyp1	acylphosphatase 1, erythrocyte (common) type	-1,5	0,047
1426801_at	39692	septin 8	-1,6	0,046
1419463_at	Clca2	chloride channel calcium activated 2	-1,6	0,036
1437341_x_at	Cnp	2',3'-cyclic nucleotide 3' phosphodiesterase	-1,6	0,044
1454930_at	Tbcel	tubulin folding cofactor E-like	-1,6	0,036
1457817_at			-1,6	0,049
1437354_at	Ube3a	ubiquitin protein ligase E3A	-1,6	0,046
1443167_at			-1,6	0,049
1423966_at	Cd99l2	CD99 antigen-like 2	-1,6	0,044
1436212_at	Tmem71	transmembrane protein 71	-1,6	0,035
1423306_at	2010002N04Rik	RIKEN cDNA 2010002N04 gene	-1,6	0,047
1425206_a_at	Ube3a	ubiquitin protein ligase E3A	-1,6	0,049
1417619_at	Gadd45gip1	growth arrest and DNA-damage-inducible, gamma interacting protein 1	-1,6	0,050
1417176_at	Csnk1e	casein kinase 1, epsilon	-1,6	0,048
1460486_at	Rabgap1	RAB GTPase activating protein 1	-1,6	0,049
1443894_at	Evi2a	ecotropic viral integration site 2a	-1,6	0,036
1428850_x_at	Cd99	CD99 antigen	-1,6	0,044
1453761_at	Phf6	PHD finger protein 6	-1,6	0,047
1433496_at	Glt25d1	glycosyltransferase 25 domain	-1,6	0,047

		containing 1		
1426555_at	Scpep1	serine carboxypeptidase 1	-1,6	0,041
1418513_at	Stk3	serine/threonine kinase 3 (Ste20, yeast homolog)	-1,6	0,049
1452888_at	1110034G24Rik	RIKEN cDNA 1110034G24 gene	-1,6	0,050
1451249_at	Trmt1	TRM1 tRNA methyltransferase 1 homolog (S. cerevisiae)	-1,6	0,048
1420975_at	Baz1b	bromodomain adjacent to zinc finger domain, 1B	-1,6	0,044
1439305_at			-1,6	0,036
1456064_at	Kcna3	potassium voltage-gated channel, shaker-related subfamily, member 3	-1,6	0,049
1451920_a_at	Rfc1	replication factor C (activator 1) 1	-1,6	0,047
1429847_a_at	4833418A01Rik	RIKEN cDNA 4833418A01 gene	-1,6	0,047
1425338_at	Plcb4	phospholipase C, beta 4	-1,6	0,047
1431430_s_at	Trim59	tripartite motif-containing 59	-1,6	0,045
1453485_s_at	1110005A03Rik	RIKEN cDNA 1110005A03 gene	-1,6	0,044
1425986_a_at	Dcun1d1	DCN1, defective in cullin neddylation 1, domain containing 1 (S. cerevisiae)	-1,6	0,047
1428900_s_at	Mett5d1	methyltransferase 5 domain containing 1	-1,6	0,049
1449749_s_at	Tfb1m	transcription factor B1, mitochondrial	-1,6	0,050
1451730_at	Zfp62	zinc finger protein 62	-1,6	0,047
1417419_at	Ccnd1	cyclin D1	-1,6	0,035
1450377_at	Thbs1	thrombospondin 1	-1,6	0,035
1421018_at	1110018J18Rik	RIKEN cDNA 1110018J18 gene	-1,6	0,047
1418980_a_at	Cnp	2',3'-cyclic nucleotide 3' phosphodiesterase	-1,6	0,050
1419279_at	Pip4k2a	phosphatidylinositol-5-phosphate 4-kinase, type II, alpha	-1,6	0,039
1426550_at	Sidt1	SID1 transmembrane family, member 1	-1,6	0,044
1450095_a_at	Acyp1	acylphosphatase 1, erythrocyte (common) type	-1,6	0,047
1434450_s_at	Adrbk2	adrenergic receptor kinase, beta 2	-1,7	0,049

1460468_s_at	Dnajc22	DnaJ (Hsp40) homolog, subfamily C, member 22	-1,7	0,035
1417568_at	Ncald	neurocalcin delta	-1,7	0,049
1451386_at	Blvrb	biliverdin reductase B (flavin reductase (NADPH))	-1,7	0,046
1448277_at	Pold2	polymerase (DNA directed), delta 2, regulatory subunit	-1,7	0,036
1433485_x_at	Gpr56	G protein-coupled receptor 56	-1,7	0,047
1448288_at	Nfib	nuclear factor I/B	-1,7	0,044
1446508_at			-1,7	0,047
1425477_x_at	H2-Ab1	histocompatibility 2, class II antigen A, beta 1	-1,7	0,047
1433466_at	AI467606	expressed sequence AI467606	-1,7	0,044
1439819_at	AU015263	expressed sequence AU015263	-1,7	0,047
1419247_at	Rgs2	regulator of G-protein signaling 2	-1,7	0,049
1455095_at	Hist2h2be	histone cluster 2, H2be	-1,7	0,050
1427680_a_at	Nfib	nuclear factor I/B	-1,7	0,049
1448012_at	C76336	expressed sequence C76336	-1,7	0,050
1454850_at	Tbc1d10c	TBC1 domain family, member 10c	-1,7	0,048
1436515_at	Bach2	BTB and CNC homology 2	-1,7	0,048
1418776_at	5830443L24Rik	RIKEN cDNA 5830443L24 gene	-1,7	0,048
1442325_at	Tbc1d24	TBC1 domain family, member 24	-1,7	0,035
1443353_at			-1,8	0,048
1417852_x_at	Clca1	chloride channel calcium activated 1	-1,8	0,047
1436171_at	Arhgap30	Rho GTPase activating protein 30	-1,8	0,035
1448482_at	Slc39a8	solute carrier family 39 (metal ion transporter), member 8	-1,8	0,049
1425396_a_at	Lck	lymphocyte protein tyrosine kinase	-1,8	0,040
1437756_at	Gimap9	GTPase, IMAP family member 9	-1,8	0,047
1425247_a_at	Igh	immunoglobulin heavy chain complex	-1,8	0,016
1418181_at	Ptp4a3	protein tyrosine phosphatase 4a3	-1,8	0,045
1417219_s_at	Tmsb10	thymosin, beta 10	-1,8	0,047
1425854_x_at	Tcrb-J	T-cell receptor beta, joining region	-1,8	0,035

1442338_at			-1,9	0,047
1458299_s_at	Nfkbie	nuclear factor of kappa light polypeptide gene enhancer in B-cells inhibitor, epsilon	-1,9	0,044
1429672_at	5830407E08Rik	RIKEN cDNA 5830407E08 gene	-1,9	0,035
1460279_a_at	Gtf2i	general transcription factor II I	-1,9	0,047
1420653_at	Tgfb1	transforming growth factor, beta 1	-1,9	0,044
1448698_at	Ccnd1	cyclin D1	-1,9	0,036
1420643_at	Lfng	LFNG O-fucosylpeptide 3-beta-N-acetylglucosaminyltransferase	-1,9	0,048
1416021_a_at	Fabp5	fatty acid binding protein 5, epidermal	-2,0	0,050
1423847_at	Ncapd2	non-SMC condensin I complex, subunit D2	-2,0	0,050
1423520_at	Lmnb1	lamin B1	-2,0	0,005
1448117_at	Kitl	kit ligand	-2,0	0,049
1436902_x_at	Tmsb10	thymosin, beta 10	-2,0	0,037
1417420_at	Ccnd1	cyclin D1	-2,0	0,049
1449005_at	Slc16a3	solute carrier family 16 (monocarboxylic acid transporters), member 3	-2,0	0,049
1450648_s_at	Rmcs5	response to metastatic cancers 5	-2,1	0,049
1438858_x_at	H2-Aa	histocompatibility 2, class II antigen A, alpha	-2,1	0,049
1417025_at	H2-Eb1	histocompatibility 2, class II antigen E beta	-2,1	0,050
1419248_at	Rgs2	regulator of G-protein signaling 2	-2,1	0,047
1450379_at	Msn	moesin	-2,1	0,047
1429065_at	1200009F10Rik	RIKEN cDNA 1200009F10 gene	-2,1	0,044
1416022_at	Fabp5	fatty acid binding protein 5, epidermal	-2,1	0,039
1419647_a_at	Ier3	immediate early response 3	-2,2	0,034
1447774_x_at	5730469M10Rik	RIKEN cDNA 5730469M10 gene	-2,2	0,048
1434067_at	AI662270	expressed sequence AI662270	-2,2	0,047
1430388_a_at	Sulf2	sulfatase 2	-2,2	0,035

1417290_at	Lrg1	leucine-rich alpha-2-glycoprotein 1	-2,2	0,036
1419004_s_at	Bcl2a1a	B-cell leukemia/lymphoma 2 related protein A1a	-2,2	0,039
1419480_at	Sell	selectin, lymphocyte	-2,2	0,039
1454268_a_at	Cyba	cytochrome b-245, alpha polypeptide	-2,2	0,036
1418296_at	Fxyd5	FXYD domain-containing ion transport regulator 5	-2,2	0,047
1433783_at	Ldb3	LIM domain binding 3	-2,3	0,049
1452716_at	5730469M10Rik	RIKEN cDNA 5730469M10 gene	-2,3	0,047
1460259_s_at	Clca2	chloride channel calcium activated 2	-2,3	0,045
1415854_at	Kitl	kit ligand	-2,3	0,047
1452431_s_at	H2-Aa	histocompatibility 2, class II antigen A, alpha	-2,5	0,047
1419549_at	Arg1	arginase, liver	-2,5	0,050
1419186_a_at	St8sia4	ST8 alpha-N-acetyl-neuraminide alpha-2,8-sialyltransferase 4	-2,5	0,047
1455966_s_at	Nudt21	nudix (nucleoside diphosphate linked moiety X)-type motif 21	-2,5	0,049
1451721_a_at	H2-Ab1	histocompatibility 2, class II antigen A, beta 1	-2,6	0,045
1436713_s_at	Meg3	maternally expressed 3	-2,6	0,046
1440196_at			-2,6	0,027
1449071_at	Myl7	myosin, light polypeptide 7, regulatory	-2,7	0,048
1424375_s_at	Gimap4	GTPase, IMAP family member 4	-2,8	0,050
1415983_at	Lcp1	lymphocyte cytosolic protein 1	-2,9	0,047
1420699_at	Clec7a	C-type lectin domain family 7, member a	-3,1	0,035
1448710_at	Cxcr4	chemokine (C-X-C motif) receptor 4	-3,1	0,022
1424931_s_at	Igl-V1	immunoglobulin lambda chain, variable 1	-3,3	0,049
1450792_at	Tyrobp	TYRO protein tyrosine kinase binding protein	-3,4	0,036
1455269_a_at	Coro1a	coronin, actin binding protein 1A	-3,5	0,049

1448617_at	Cd53	CD53 antigen	-3,7	0,047
1452163_at	Ets1	E26 avian leukemia oncogene 1, 5' domain	-3,9	0,044
1460218_at	Cd52	CD52 antigen	-4,0	0,044
1416246_a_at	Coro1a	coronin, actin binding protein 1A	-4,5	0,039
1417426_at	Srgn	serglycin	-4,6	0,050
1427747_a_at	Lcn2	lipocalin 2	-4,8	0,047
1460423_x_at	Igkv1-117	immunoglobulin kappa chain variable 1-117	-5,5	0,035
1455869_at			-6,2	0,047

List of differentially expressed genes assessed using the limma package from Bioconductor (Fold change>1.5 and adjusted p-value<0.05)

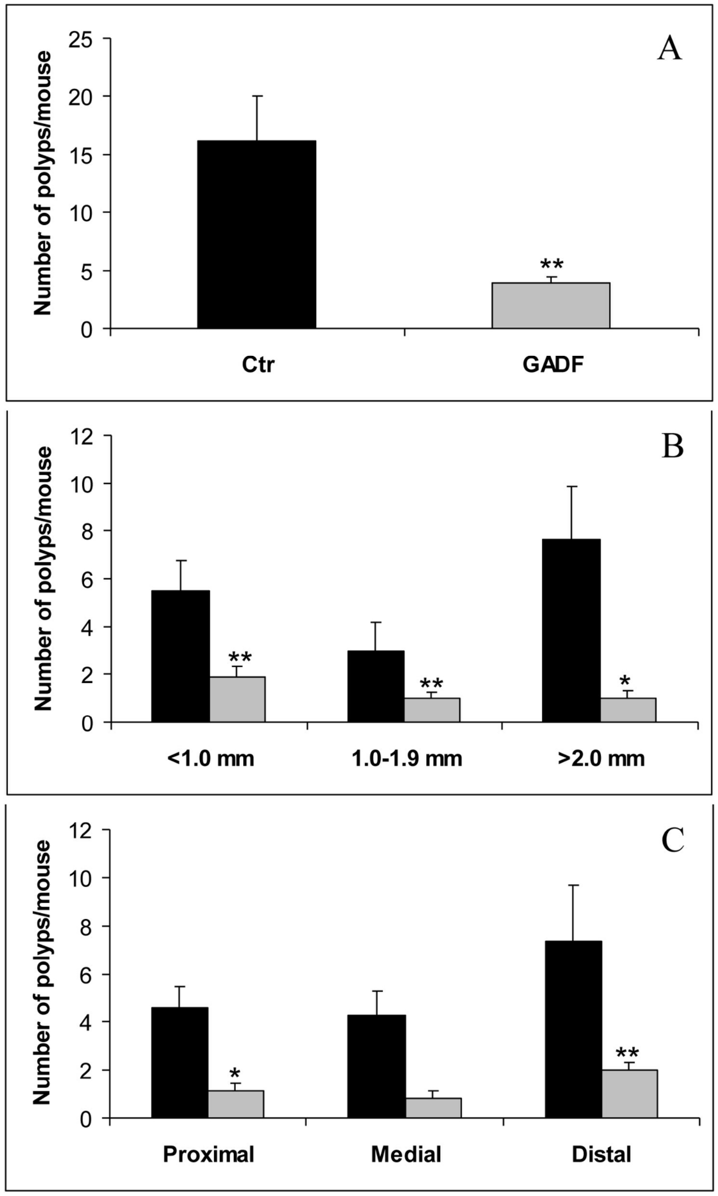

Fig. 1. A) Total number of polyps/mouse in the small intestine of Apc$^{Min/+}$ mice. B) Number of polyps/mouse in proximal, medial and distal sections. C) Number of polyps/mouse shown by polyp size distribution (<1 mm diameter polyps, 1–2 mm and >2 mm). Data represented as mean ± SEM (*, $p > 0.05$) (* *, $p > 0.01$).
147x209mm (300 x 300 DPI)

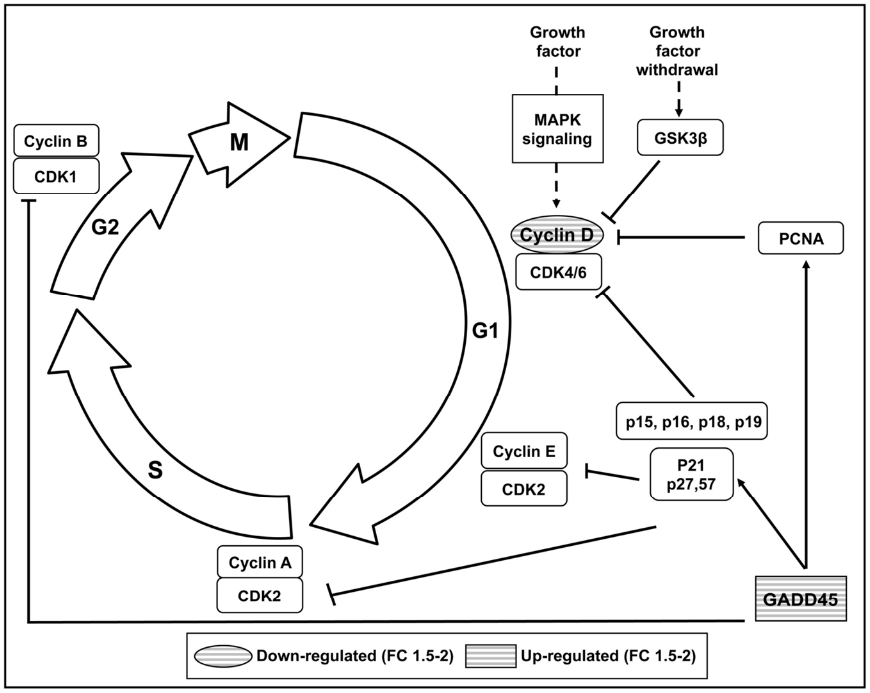

Fig. 2. Adaptation of KEGG cell cycle pathway using KEGG Mapper. Oval pathway members were significantly down-regulated and rectangular members were found to be up-regulated in the intestinal mucosa of $Apc^{Min/+}$ mice treated with GADF. Horizontal lines indicate a fold change (FC) of between 1.5 and 2.
147x104mm (300 x 300 DPI)

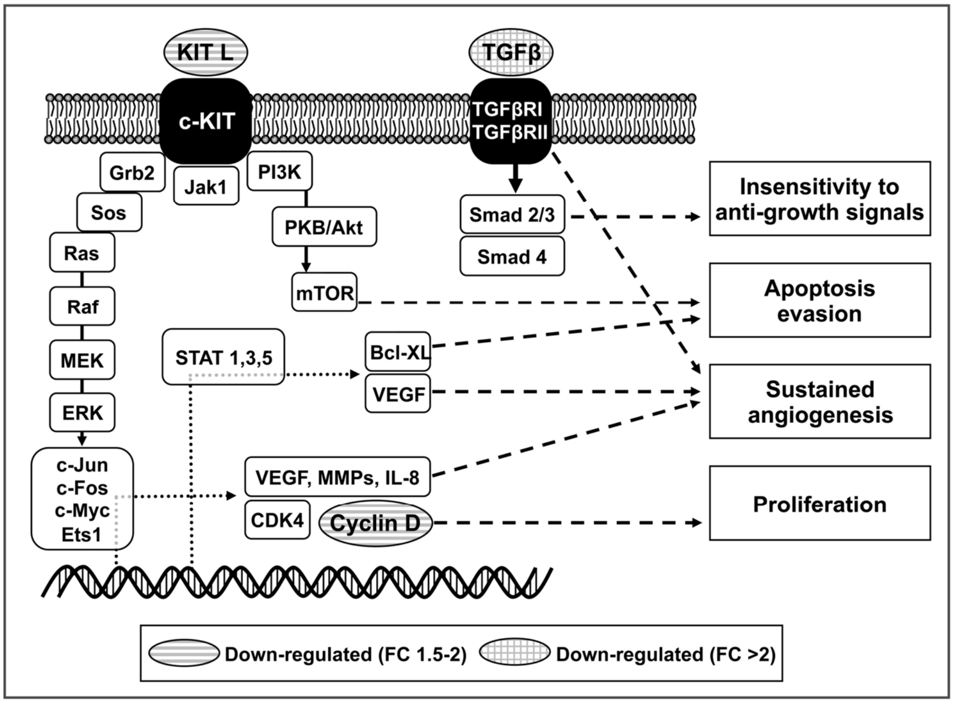

Fig. 3. Adaptation of KEGG pathways in cancer using KEGG Mapper. Ovals represent down-regulated genes following GADF supplementation. Horizontal lines indicate a FC of between 1.5 and 2 and vertical lines specify a FC of more than 2.
147x104mm (300 x 300 DPI)

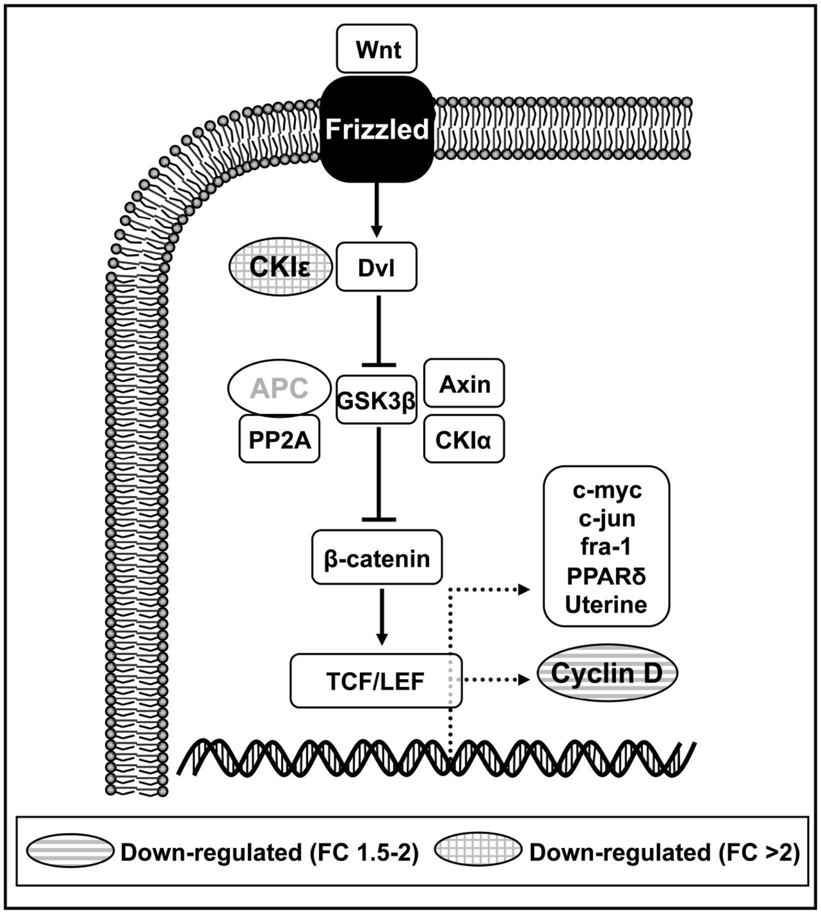

Fig. 4. Adaptation of KEGG Wnt signaling pathway using KEGG Mapper. Ovals represent down-regulated genes encoding that protein in $Apc^{Min/+}$ mice following GADF treatment. Horizontal lines indicate a FC in expression of between 1.5 and 2 and vertical lines specify a FC of more than 2.

209x297mm (300 x 300 DPI)

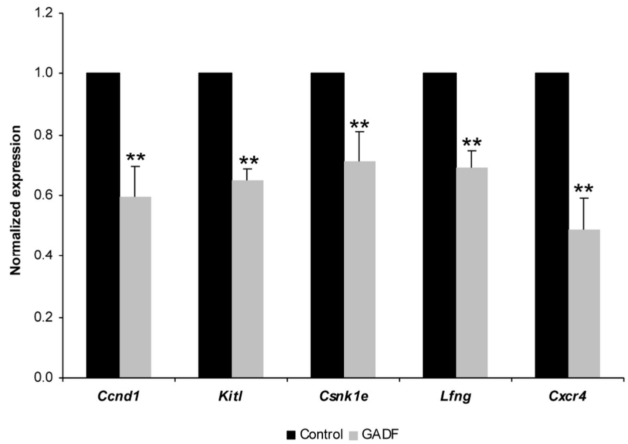

Fig. 5. Validation of genes that were differentially expressed in the colon mucosa of Apc$^{Min/+}$ mice after GADF treatment by RT-PCR. Data represented as mean ± SEM (* *, $p > 0.01$).
209x147mm (300 x 300 DPI)

Supplemental table 1. Differentially expressed genes by GADF treatment in the colon mucosa of APC$^{Min/+}$ mice

Affimetrix ID	Gene Symbol	Gene description	Fold change	Adjusted p-value
1418283_at	Cldn4	claudin 4	2,0	0,047
1449133_at	Sprr1a	small proline-rich protein 1A	2,0	0,035
1451924_a_at	Edn1	endothelin 1	1,9	0,049
1419911_at	Coro1c	coronin, actin binding protein 1C	1,8	0,047
1443208_at			1,8	0,035
1441115_at	D18Ertd232e	DNA segment, Chr 18, ERATO Doi 232, expressed	1,8	0,041
1439124_at	Wdr91	WD repeat domain 91	1,8	0,049
1417133_at	Pmp22	peripheral myelin protein 22	1,7	0,022
1433205_at	Ndfip2	Nedd4 family interacting protein 2	1,7	0,039
1436520_at	Ahnak2	AHNAK nucleoprotein 2	1,7	0,044
1436750_a_at	Oxct1	3-oxoacid CoA transferase 1	1,7	0,049
1424339_at	Oasl1	2'-5' oligoadenylate synthetase-like 1	1,7	0,036
1455180_at	Gcom1	GRINL1A complex locus	1,7	0,047
1455457_at	Cyp2c54	cytochrome P450, family 2, subfamily c, polypeptide 54	1,7	0,049
1436614_at			1,7	0,046
1430191_at	9130004J05Rik	RIKEN cDNA 9130004J05 gene	1,7	0,045
1434496_at	Plk3	polo-like kinase 3 (Drosophila)	1,7	0,022
1458279_at			1,7	0,022
1455804_x_at	Oxct1	3-oxoacid CoA transferase 1	1,6	0,049
1422823_at	Eps8	epidermal growth factor receptor pathway substrate 8	1,6	0,044
1441030_at	Rai14	retinoic acid induced 14	1,6	0,044
1426818_at	Arrdc4	arrestin domain containing 4	1,6	0,035
1437868_at	Fam46a	family with sequence similarity 46, member A	1,6	0,035
1435059_at	Asap1	ArfGAP with SH# domain, ankyrin repeat and PH domain1	1,6	0,036
1436101_at	Pank2	pantothenate kinase 2 (Hallervorden-Spatz syndrome)	1,6	0,047
1438581_at	Cytsa	cytospin A	1,6	0,047
1425837_a_at	Ccrn4l	CCR4 carbon catabolite repression 4-like (S. cerevisiae)	1,6	0,049
1417732_at	Anxa8	annexin A8	1,6	0,049
1421151_a_at	Epha2	Eph receptor A2	1,6	0,035
1439598_at			1,5	0,036

1458591_at	Rasef	RAS and EF hand domain containing	1,5	0,044
1417335_at	Sult2b1	sulfotransferase family, cytosolic, 2B, member 1	1,5	0,049
1452385_at	Usp53	ubiquitin specific peptidase 53	1,5	0,044
1449519_at	Gadd45a	growth arrest and DNA-damage-inducible 45 alpha	1,5	0,050
1448873_at	Ocln	occludin	1,5	0,044
1455033_at	Fam102b	family with sequence similarity 102, member B	1,5	0,047
1426894_s_at	Fam102a	family with sequence similarity 102, member A	1,5	0,049
1435265_at			1,5	0,035
1458453_at	Lmo7	LIM domain only 7	1,5	0,048
1422824_s_at	Eps8	epidermal growth factor receptor pathway substrate 8	1,5	0,049
1418459_at	Ccdc91	coiled-coil domain containing 91	-1,5	0,035
1420249_s_at	Ccl6	chemokine (C-C motif) ligand 6	-1,5	0,049
1449342_at	Ptplb	protein tyrosine phosphatase-like (proline instead of catalytic arginine), member b	-1,5	0,047
1452191_at	Prcp	prolylcarboxypeptidase (angiotensinase C)	-1,5	0,047
1430514_a_at	Cd99	CD99 antigen	-1,5	0,044
1430656_a_at	Asnsd1	asparagine synthetase domain containing 1	-1,5	0,049
1435864_a_at	1810063B05Rik	RIKEN cDNA 1810063B05 gene	-1,5	0,047
1451091_at	Txndc5	thioredoxin domain containing 5	-1,5	0,049
1433831_at	4833418A01Rik	RIKEN cDNA 4833418A01 gene	-1,5	0,047
1422029_at	Ccl20	chemokine (C-C motif) ligand 20	-1,5	0,049
1451987_at	Arrb2	arrestin, beta 2	-1,5	0,035
1428340_s_at	Atp13a2	ATPase type 13A2	-1,5	0,039
1453550_a_at	Far1	fatty acyl CoA reductase 1	-1,5	0,036
1436038_a_at	Pigp	phosphatidylinositol glycan anchor biosynthesis, class P	-1,5	0,049
1434955_at	March1	membrane-associated ring finger (C3HC4) 1	-1,5	0,049
1421022_x_at	Acyp1	acylphosphatase 1, erythrocyte (common) type	-1,5	0,047
1426801_at	39692	septin 8	-1,6	0,046
1419463_at	Clca2	chloride channel calcium activated 2	-1,6	0,036
1437341_x_at	Cnp	2',3'-cyclic nucleotide 3' phosphodiesterase	-1,6	0,044
1454930_at	Tbcel	tubulin folding cofactor E-like	-1,6	0,036
1457817_at			-1,6	0,049
1437354_at	Ube3a	ubiquitin protein ligase E3A	-1,6	0,046

1443167_at			-1,6	0,049
1423966_at	Cd99l2	CD99 antigen-like 2	-1,6	0,044
1436212_at	Tmem71	transmembrane protein 71	-1,6	0,035
1423306_at	2010002N04Rik	RIKEN cDNA 2010002N04 gene	-1,6	0,047
1425206_a_at	Ube3a	ubiquitin protein ligase E3A	-1,6	0,049
1417619_at	Gadd45gip1	growth arrest and DNA-damage-inducible, gamma interacting protein 1	-1,6	0,050
1417176_at	Csnk1e	casein kinase 1, epsilon	-1,6	0,048
1460486_at	Rabgap1	RAB GTPase activating protein 1	-1,6	0,049
1443894_at	Evi2a	ecotropic viral integration site 2a	-1,6	0,036
1428850_x_at	Cd99	CD99 antigen	-1,6	0,044
1453761_at	Phf6	PHD finger protein 6	-1,6	0,047
1433496_at	Glt25d1	glycosyltransferase 25 domain containing 1	-1,6	0,047
1426555_at	Scpep1	serine carboxypeptidase 1	-1,6	0,041
1418513_at	Stk3	serine/threonine kinase 3 (Ste20, yeast homolog)	-1,6	0,049
1452888_at	1110034G24Rik	RIKEN cDNA 1110034G24 gene	-1,6	0,050
1451249_at	Trmt1	TRM1 tRNA methyltransferase 1 homolog (S. cerevisiae)	-1,6	0,048
1420975_at	Baz1b	bromodomain adjacent to zinc finger domain, 1B	-1,6	0,044
1439305_at			-1,6	0,036
1456064_at	Kcna3	potassium voltage-gated channel, shaker-related subfamily, member 3	-1,6	0,049
1451920_a_at	Rfc1	replication factor C (activator 1) 1	-1,6	0,047
1429847_a_at	4833418A01Rik	RIKEN cDNA 4833418A01 gene	-1,6	0,047
1425338_at	Plcb4	phospholipase C, beta 4	-1,6	0,047
1431430_s_at	Trim59	tripartite motif-containing 59	-1,6	0,045
1453485_s_at	1110005A03Rik	RIKEN cDNA 1110005A03 gene	-1,6	0,044
1425986_a_at	Dcun1d1	DCN1, defective in cullin neddylation 1, domain containing 1 (S. cerevisiae)	-1,6	0,047
1428900_s_at	Mett5d1	methyltransferase 5 domain containing 1	-1,6	0,049
1449749_s_at	Tfb1m	transcription factor B1, mitochondrial	-1,6	0,050
1451730_at	Zfp62	zinc finger protein 62	-1,6	0,047
1417419_at	Ccnd1	cyclin D1	-1,6	0,035
1450377_at	Thbs1	thrombospondin 1	-1,6	0,035
1421018_at	1110018J18Rik	RIKEN cDNA 1110018J18 gene	-1,6	0,047
1418980_a_at	Cnp	2',3'-cyclic nucleotide 3' phosphodiesterase	-1,6	0,050

1419279_at	Pip4k2a	phosphatidylinositol-5-phosphate 4-kinase, type II, alpha	-1,6	0,039
1426550_at	Sidt1	SID1 transmembrane family, member 1	-1,6	0,044
1450095_a_at	Acyp1	acylphosphatase 1, erythrocyte (common) type	-1,6	0,047
1434450_s_at	Adrbk2	adrenergic receptor kinase, beta 2	-1,7	0,049
1460468_s_at	Dnajc22	DnaJ (Hsp40) homolog, subfamily C, member 22	-1,7	0,035
1417568_at	Ncald	neurocalcin delta	-1,7	0,049
1451386_at	Blvrb	biliverdin reductase B (flavin reductase (NADPH))	-1,7	0,046
1448277_at	Pold2	polymerase (DNA directed), delta 2, regulatory subunit	-1,7	0,036
1433485_x_at	Gpr56	G protein-coupled receptor 56	-1,7	0,047
1448288_at	Nfib	nuclear factor I/B	-1,7	0,044
1446508_at			-1,7	0,047
1425477_x_at	H2-Ab1	histocompatibility 2, class II antigen A, beta 1	-1,7	0,047
1433466_at	AI467606	expressed sequence AI467606	-1,7	0,044
1439819_at	AU015263	expressed sequence AU015263	-1,7	0,047
1419247_at	Rgs2	regulator of G-protein signaling 2	-1,7	0,049
1455095_at	Hist2h2be	histone cluster 2, H2be	-1,7	0,050
1427680_a_at	Nfib	nuclear factor I/B	-1,7	0,049
1448012_at	C76336	expressed sequence C76336	-1,7	0,050
1454850_at	Tbc1d10c	TBC1 domain family, member 10c	-1,7	0,048
1436515_at	Bach2	BTB and CNC homology 2	-1,7	0,048
1418776_at	5830443L24Rik	RIKEN cDNA 5830443L24 gene	-1,7	0,048
1442325_at	Tbc1d24	TBC1 domain family, member 24	-1,7	0,035
1443353_at			-1,8	0,048
1417852_x_at	Clca1	chloride channel calcium activated 1	-1,8	0,047
1436171_at	Arhgap30	Rho GTPase activating protein 30	-1,8	0,035
1448482_at	Slc39a8	solute carrier family 39 (metal ion transporter), member 8	-1,8	0,049
1425396_a_at	Lck	lymphocyte protein tyrosine kinase	-1,8	0,040
1437756_at	Gimap9	GTPase, IMAP family member 9	-1,8	0,047
1425247_a_at	Igh	immunoglobulin heavy chain complex	-1,8	0,016
1418181_at	Ptp4a3	protein tyrosine phosphatase 4a3	-1,8	0,045
1417219_s_at	Tmsb10	thymosin, beta 10	-1,8	0,047
1425854_x_at	Tcrb-J	T-cell receptor beta, joining region	-1,8	0,035

1442338_at			-1,9	0,047
1458299_s_at	Nfkbie	nuclear factor of kappa light polypeptide gene enhancer in B-cells inhibitor, epsilon	-1,9	0,044
1429672_at	5830407E08Rik	RIKEN cDNA 5830407E08 gene	-1,9	0,035
1460279_a_at	Gtf2i	general transcription factor II I	-1,9	0,047
1420653_at	Tgfb1	transforming growth factor, beta 1	-1,9	0,044
1448698_at	Ccnd1	cyclin D1	-1,9	0,036
1420643_at	Lfng	LFNG O-fucosylpeptide 3-beta-N-acetylglucosaminyltransferase	-1,9	0,048
1416021_a_at	Fabp5	fatty acid binding protein 5, epidermal	-2,0	0,050
1423847_at	Ncapd2	non-SMC condensin I complex, subunit D2	-2,0	0,050
1423520_at	Lmnb1	lamin B1	-2,0	0,005
1448117_at	Kitl	kit ligand	-2,0	0,049
1436902_x_at	Tmsb10	thymosin, beta 10	-2,0	0,037
1417420_at	Ccnd1	cyclin D1	-2,0	0,049
1449005_at	Slc16a3	solute carrier family 16 (monocarboxylic acid transporters), member 3	-2,0	0,049
1450648_s_at	Rmcs5	response to metastatic cancers 5	-2,1	0,049
1438858_x_at	H2-Aa	histocompatibility 2, class II antigen A, alpha	-2,1	0,049
1417025_at	H2-Eb1	histocompatibility 2, class II antigen E beta	-2,1	0,050
1419248_at	Rgs2	regulator of G-protein signaling 2	-2,1	0,047
1450379_at	Msn	moesin	-2,1	0,047
1429065_at	1200009F10Rik	RIKEN cDNA 1200009F10 gene	-2,1	0,044
1416022_at	Fabp5	fatty acid binding protein 5, epidermal	-2,1	0,039
1419647_a_at	Ier3	immediate early response 3	-2,2	0,034
1447774_x_at	5730469M10Rik	RIKEN cDNA 5730469M10 gene	-2,2	0,048
1434067_at	AI662270	expressed sequence AI662270	-2,2	0,047
1430388_a_at	Sulf2	sulfatase 2	-2,2	0,035
1417290_at	Lrg1	leucine-rich alpha-2-glycoprotein 1	-2,2	0,036
1419004_s_at	Bcl2a1a	B-cell leukemia/lymphoma 2 related protein A1a	-2,2	0,039
1419480_at	Sell	selectin, lymphocyte	-2,2	0,039
1454268_a_at	Cyba	cytochrome b-245, alpha polypeptide	-2,2	0,036
1418296_at	Fxyd5	FXYD domain-containing ion transport regulator 5	-2,2	0,047
1433783_at	Ldb3	LIM domain binding 3	-2,3	0,049
1452716_at	5730469M10Rik	RIKEN cDNA 5730469M10 gene	-2,3	0,047

1460259_s_at	Clca2	chloride channel calcium activated 2	-2,3	0,045
1415854_at	Kitl	kit ligand	-2,3	0,047
1452431_s_at	H2-Aa	histocompatibility 2, class II antigen A, alpha	-2,5	0,047
1419549_at	Arg1	arginase, liver	-2,5	0,050
1419186_a_at	St8sia4	ST8 alpha-N-acetyl-neuraminide alpha-2,8-sialyltransferase 4	-2,5	0,047
1455966_s_at	Nudt21	nudix (nucleoside diphosphate linked moiety X)-type motif 21	-2,5	0,049
1451721_a_at	H2-Ab1	histocompatibility 2, class II antigen A, beta 1	-2,6	0,045
1436713_s_at	Meg3	maternally expressed 3	-2,6	0,046
1440196_at			-2,6	0,027
1449071_at	Myl7	myosin, light polypeptide 7, regulatory	-2,7	0,048
1424375_s_at	Gimap4	GTPase, IMAP family member 4	-2,8	0,050
1415983_at	Lcp1	lymphocyte cytosolic protein 1	-2,9	0,047
1420699_at	Clec7a	C-type lectin domain family 7, member a	-3,1	0,035
1448710_at	Cxcr4	chemokine (C-X-C motif) receptor 4	-3,1	0,022
1424931_s_at	Igl-V1	immunoglobulin lambda chain, variable 1	-3,3	0,049
1450792_at	Tyrobp	TYRO protein tyrosine kinase binding protein	-3,4	0,036
1455269_a_at	Coro1a	coronin, actin binding protein 1A	-3,5	0,049
1448617_at	Cd53	CD53 antigen	-3,7	0,047
1452163_at	Ets1	E26 avian leukemia oncogene 1, 5' domain	-3,9	0,044
1460218_at	Cd52	CD52 antigen	-4,0	0,044
1416246_a_at	Coro1a	coronin, actin binding protein 1A	-4,5	0,039
1417426_at	Srgn	serglycin	-4,6	0,050
1427747_a_at	Lcn2	lipocalin 2	-4,8	0,047
1460423_x_at	Igkv1-117	immunoglobulin kappa chain variable 1-117	-5,5	0,035
1455869_at			-6,2	0,047

List of differentially expressed genes assessed using the limma package from Bioconductor (Fold change>1.5 and adjusted p-value<0.05)